JOURNAL OF SOLID STATE CHEMISTRY 117, 343–350 (1995)

Homogeneity-Related Problems in Solution Derived Powders

P. Barboux, P. Griesmar, F. Ribot, and L. Mazerolles*

*Chimie de la Matière Condensée, Université Pierre et Marie Curie, 4 Place Jussieu, 75252 Paris Cedex 05, France; and *Centre d'Etude de Chimie Métallurgique, 15 Rue Georges Urbain, 94400 Vitry sur Seine, France*

Received August 28, 1994; in revised form February 2, 1995; accepted February 3, 1995

The role of homogeneity in the reactivity of multicomponent powders resulting from solution synthesis is discussed. Examples have been given in perovskite-derived systems, such as superconducting cuprates and ferroelectric $PbTi_{1-x}Zr_xO_3$, which are of technological interest. Also, metastable structures may be obtained by low-temperature synthesis, as observed in the $PbO–ZrO_2$ system. In this system, we discuss the opposing effects of homogeneity and diffusion kinetics during the calcination steps and heating process. © 1995 Academic Press, Inc.

INTRODUCTION

Solution processes have been extensively used in recent years to produce ceramic powders, films, or fibers (1). Mixing at the molecular level and the possibility of using organic ligands to tailor the reactivity of the precursors and the morphology of the inorganic polymers have allowed the production of improved ceramics through better control of the precursor chemistry. Most of the precursors used are metal alkoxides, $M(OR)_n$, which undergo polymerization upon hydrolysis (1). However, the high cost of these alkoxide precursors, as well as the difficulty in handling them, is in most cases a formidable drawback to any application. Most of the recent research has then turned to the synthesis of multielement ceramics with high value in advanced technological applications such as electronics, membranes, sensors, or various coatings (2). These applications often involve integration into a system as a coating (3), but reaction with the substrate is always difficult to deal with, whether it is interesting for texturing purposes or deleterious at the interface. Therefore, most of the effort in solution chemistry is based on the potential lowering of the crystallization temperature. This can be obtained only if complete homogeneity of all elements is achieved at the molecular scale throughout the processes of mixing in solution and condensation of the oxo-polymer, as well as during drying and calcination steps up to the crystallization temperature.

In these systems, the crystallization mechanism appears to be of great interest. In the case of a homogeneous amorphous film, the crystallization may be controlled by nucleation that may be favored at the interface with the substrate. But in a heterogeneous film, crystallization of a multicomponent phase will only occur through solid state diffusion reactions between nanometric particles. In the first case we should expect textured films to crystallize whereas polycrystalline films should be obtained in the second case.

This is not restricted to solution synthesis of thin films and many results can be also obtained from other thin film evaporation techniques (sputtering, laser, etc.) in which elements are simultaneously deposited onto a hot substrate. In these methods, multielement oxide materials, such as $YBa_2Cu_3O_7$ or $PbZr_{1-x}Ti_xO_3$, can be obtained with a high degree of orientation at temperatures as low as 500–600°C when homogeneously deposited and annealed *in situ* during the deposition, whereas they can be synthesized only above 900°C using conventional solid state methods or post-deposition annealings.

Of course, the problem of low-temperature synthesis is not limited to films only and it is strongly related to the synthesis of bulk materials, especially metastable compounds. Since most of the classical solid state reactions are diffusion-controlled, they require high reaction temperatures because of limited solid state diffusion. Therefore only systems of phases stable both from the thermodynamics and from the diffusion point of view can be obtained. Under synthesis conditions controlled by diffusion, metastable phases, which are thermodynamically stable but not stable against diffusion, cannot be obtained. Therefore, much research has been associated with the synthesis of reactive molecular precursors for low-temperature phases.

Many works have dealt with the chemistry of the solution precursors, their hydrolysis, and the first condensation steps that lead to the oligomeric species. But very few studies have addressed the problem of controlling the homogeneity and the reactivity of the resulting powders during the heating process. Some questions of great im-

0022-4596/95 $12.00

portance remain, such as how homogeneous the mixture must be and what the relationship is between homogeneity and reactivity.

This paper is divided into two parts. In the first, we discuss the role of homogeneity in lowering the reaction temperature and reaction time of both films and powders. In the second part, we illustrate the discussion with experimental results related to the synthesis of the $PbZrO_3$ perovskite.

1. HOMOGENEITY AND REACTIVITY

1.1. Mixing Scale and Diffusion Range

At first sight, the best way to obtain a reactive mixture is to start from homogeneous precursors in solution that have already formed stable bridging oxygen bonds between each component. A large number of syntheses of such mixed alkoxides have been recently reviewed (4, 5). They allow the low-temperature synthesis of binary systems, such as ferroelectric perovskite-derived phases $PbZr_{1-x}Ti_xO_3$ (5, 6) or $LiNbO_3$ (7). But these examples may be favorable cases where the phase would still form without difficulty from a heterogeneous mixture. The crystallization of a similar material, $BaTiO_3$, is obtained by refluxing a Ba–Ti alkoxide mixture for a few days at 90°C in a basic solution without a specific heteroalkoxide (8). Similarly, for the synthesis of $PbTiO_3$, we have used a method based on the reaction of lead acetate with titanium alkoxide (9). No heteroalkoxide is obtained and the ^1H and ^{13}C NMR spectra of these materials obtained with various Pb/Ti ratios clearly demonstrate that a lead alkoxide is formed imbedded in a polymeric titanium oxoacetate but no Pb–O–Ti linkage is formed (10). Hydrolysis leads to the precipitation of an amorphous powder that crystallizes at low temperature (350°C). This is an indication that, in this particular case, the binary system forms at low temperature because it is the stable form and that for crystallization to occur at these low temperatures, it is sufficient that homogeneity be obtained at low scale although not at molecular scale (9, 11).

Moreover, it has not yet been demonstrated that the crystalline structures proposed for heteroalkoxides remain stable in the solution, and that they will withstand the hydrolysis, drying, and calcination steps without phase separation. Indeed, amorphous mixtures of oxides or hydroxides that result from a solution synthesis are highly unstable materials that may stabilize by crystallization but may also yield phase separation upon heating if it is favored by thermodynamics and allowed by kinetics. This will result in a heterogeneous mixture of fine powders or in nanocomposites (12).

In the case of materials with low-valent cations having high mobility, such as $YBa_2Cu_3O_7$ and $Bi_2Sr_2Ca_2Cu_3O_{10}$ superconducting cuprates, phase separation into single oxides that recombine later into binary and then ternary phases upon heating to higher temperatures is always observed. This phase decomposition results in a final temperature of heating that is very high although the fine dispersion of these solution derived powders may still allow a slight decrease in the synthesis temperature. As an example, during the synthesis of the $YBaCu_3O_7$ (123) phase, coprecipitated hydroxides yield a phase separation into single oxides around 300°C and this mixture yields the pure 123 phase in 20 min at 800°C as compared to a few hours at 900°C in the conventional solid state reaction of commercial oxides and carbonates (13, 14).

In these systems, a way to decrease the synthesis temperature is to lower the temperature of formation of the ternary phase by decreasing the oxygen pressure (14). Alternatively, although the reaction temperature will not be lowered, the reaction times will be drastically decreased by rapidly heating the material to the temperature domain where the multicomponent phase is stable, as compared to reaction times at temperatures where phase separation occurs. Starting from neodecanoates of Y, Ba, and Cu, Hamdi *et al.* have succeeded in obtaining the $YBa_2Cu_3O_7$ phase within 10 sec at 900°C by rapid thermal annealing (RTA) (15). Similar results have been obtained for $PbTiO_3$ thin films (16). If we recall that the main purpose is to avoid parasitic reactions with the substrate, the reduction in reaction time might appear as important as decreasing the reaction temperature. However, the calcination of residual organics as well as the heating cycle of these fast reactions may not favor a texturing of the film by the substrate. Similarly, rapid heating of (Bi, Sr, Ca, Cu) thin oxide films prevented the thermodynamic stabilization of the system by phase separation into $Bi_2Sr_2CuO_6$ and $CaCuO_2$ that later inhibited crystallization of the quaternary phase $Bi_2Sr_2CaCu_2O_8$ superconductor (17).

In some cases, rapid heating may decrease the crystallization temperature by inhibiting the formation of an intermediary phase that stabilizes the system. This has been demonstrated in the mullite (Al_2SiO_5) system (18, 19). In this case, a parasitic tetragonal mullite related to some phase separation between Al and Si forms instead of the desired orthorhombic phase. However, rapid heating may prevent this trouble and results in a lower crystallization temperature.

Metastable structures may still crystallize at low temperatures from homogeneous mixtures if low kinetics of diffusion hinder phase separation into simple oxides. This means that short-range ordering will be preferred to long-range diffusion at low temperatures. This idea of diffusion-limited crystallization has been developed by Lange *et al.* (12).

A nice example has been provided by Bonhomme-Coury *et al.* (20). Upon heating homogeneous gels obtained by slow hydrolysis of Al and Ti alkoxides,

β-Al_2TiO_5 crystallizes at 800°C. This phase appears as a local ordering of the homogeneous mixture but is metastable and decomposes into Al_2O_3 and TiO_2 after longer times or when faster diffusion is possible at higher temperatures. It forms again above the temperature of 1280°C at which it becomes stable.

These results simply indicate that the stability of a multielement phase is not a problem for its synthesis as long as homogeneity conditions are satisfied and limited diffusion prevents phase separation. However, the concept of homogeneity scale will have to be refined in future works. On a first attempt it should combine the scale of mixing with the diffusion lengths of the elements during heating to the temperature region where the phase can form.

A metastable multicomponent structure may crystallize only if homogeneity is achieved, because of limited diffusion crystallization. In contrast, a stable structure will always form from a heterogeneous mixture as soon as the diffusion lengths (related to the temperature) are on the order of the heterogeneity distance. In this case the rates of formation will be accelerated by the homogeneity. In some cases, such as the $PbTiO_3$ perovskite, the state of dispersion will not affect the reaction mechanisms and the activation energy for crystallization. This is not the general rule, however, since in a similar but less reactive system such as $PbZrO_3$, the activation energy depends on the scale of mixing (21). Also, upon increasing the homogeneity, the diffusion-controlled reactions may transform to nucleation-controlled reactions. In this domain, interesting results have been recently obtained in multielement thin films made from superlattice composites. Depending on the thickness of the elemental layers, an amorphous ternary phase as the reaction intermediate appears more stable than the binary compounds. In these systems, which have a well-defined geometry, it is easy to identify the scale of mixing with the thickness of the elemental layers. They clearly demonstrate the effect of mixing on the crystallization pathways (22, 23).

1.2. Homogeneity and Reactivity in Ternary Systems

Homogeneity may not be the most attractive method to obtain a multielement system. When phase separation occurs in the heating process, the most stable phases form and the system loses its reactivity. Then, some specific heterogeneity is preferred in the starting precursor powder. In the synthesis of PMN ($PbMg_{0.33}Nb_{0.66}O_3$), phase separation occurs by a reaction between lead and niobium, which crystallize into a pyrochlore phase and leave MgO separate (24). The perovskite then nucleates with difficulty from the pyrochlore phase (25). Therefore, some classical solid state synthesis procedures have started from powders of $MgNb_2O_6$ mixed with PbO, because they have a higher reactivity (26). Similarly, in the most successful solution preparations, lead is added last, after the reaction of niobium precursor with magnesium alkoxide has proceeded for a long time (27).

Khan *et al.* studied the effect of the particle size of colloidal $Y(OH)_3$ used as the Y-precursor for the production of $YBa_2Cu_3O_7$ films (28). Mixing this colloidal hydroxide with a solution of copper acetate and barium hydroxide results in a polycondensation of hydroxides and acetates and a gelation (28). Fresh yttrium sols have a small particle size and dissolve completely, resulting in a polymeric gel with a high (Y–Ba–Cu) homogeneity. The larger particles of aged yttrium hydroxide sols do not completely dissolve. They result in a lower homogeneity and leave yttrium-rich particles, 1 μm in size, imbedded in a Ba–Cu polymeric gel of acetate and hydroxide. It is difficult to track the actual mechanism of the reaction, but it appears that heterogeneous gels give better results in terms of the reactivity and kinetics of formation of the superconducting phase. As an attempt at explanation we have concluded that homogeneous gels would decompose into a binary $Y_2Cu_2O_5$ phase mixed with barium carbonate. This is probably the most stable equilibrium assemblage obtained from the decomposition of the amorphous homogeneous mixture. However, the heterogeneous gel yields yttrium oxide mixed with $BaCuO_2$, which is known to be more reactive, probably because of the low melting point of $BaCuO_2$ (920°C) (29).

1.3. Crystalline Defects Resulting from Low-Temperature Synthesis

Most of the structural defects observed in phases obtained by low-temperature synthesis relate to the low diffusion kinetics. The structural ordering is achieved at short range only, resulting in small coherence domains, as observed by X-ray diffraction. As an example, the $YBa_2Cu_3O_{7-y}$ phase is a perovskite, with oxygen vacancies, characterized by an ordering of the large cations (Y and Ba) along the c axis. When it is obtained at low temperature, the structure, as shown by X-ray diffraction, has a tetragonal symmetry (14, 30) associated with a fixed oxygen composition ($y = 0.33$) and a semiconducting behavior. This has been attributed to microtwins that relate to an incomplete ordering of the Y and Ba cations (14). However, some other studies have attributed the tetragonal symmetry of the low-temperature phase to carbonates remaining in the structure (31). After annealing at 920°C and slow cooling under oxygen, the same material recovers its regular properties, such as its orthorhombic structure, its oxygen mobility, and its metallicity.

A similar disordering among the cations has been observed in the $NaMnO_2$ and in the $LiCoO_2$ structures, which are cathodic materials for secondary battery applications. In the latter case, the regular $LiCoO_2$ obtained

at high temperature by solid state synthesis has a layered hexagonal structure consisting of Li and Co cations ordered plane by plane in the octahedral sites of a cubic close-packed array of oxygen atoms. The low-temperature phase, however, exhibits a cubic symmetry similar to the spinel structure, which has a similar array of oxygen atoms but which could be explained by a partial disordering of Li and Co among cationic sites.

Another explanation is that all low-temperature synthesis methods of this material give a phase separation into a mixture containing the Co_3O_4 spinel (32, 33). Thus, the $LiCoO_2$ cubic structure may nucleate, preferentially to the hexagonal structure, at the surface of the cubic Co_3O_4 grains (34). Indeed, a similar explanation has been given by Huling and Messing for the formation of tetragonal spinel-like mullite when starting from a heterogeneous mixture of Al and Si (18). Phase separation occurs and yields γ-Al_2O_3, the spinel structure of which offers a good nucleation site for the tetragonal mullite (18).

2. SYNTHESIS OF $PbZrO_3$

We have previously investigated the $PbZr_{1-x}Ti_xO_3$ system using titanium and zirconium tetrabutoxide associated with lead alkoxide (9–11). Although the $PbTiO_3$ perovskite phase rapidly crystallizes at low temperature (300–400°C), higher synthesis temperatures are required for $PbZrO_3$, which crystallizes only above 600°C with very slow kinetics. From thermodynamic data, the $PbZrO_3$ perovskite structure is stable at room temperature toward decomposition into PbO and ZrO_2 (35). But upon heat treatment to 400°C, the amorphous mixture obtained with lead acetate and zirconium butoxide as the precursors yields a phase separation into poorly crystallized PbO and ZrO_2 (9). As mentioned above, no mixed alkoxide forms during the process. The poor reactivity may relate to the lack of homogeneity in the mixture. So the question arises of whether this phase separation is inherent in the process or in the PbO–ZrO2 system. Therefore, we have been interested in the system consisting of the isopropoxides of Zr and Pb that are known to form mixed alkoxides (36). Contrary to the lead acetate–zirconium butoxide case, this allows the study of the effects of homogeneity and of the heating process in the calcination of mixtures of zirconium and lead oxides. As a matter of fact, this system has already been described by Yamagushi *et al.* (37).

2.1. Experimental Details

Propanol-2 was distilled over sodium. Anhydrous lead acetate ($Pb(CH_3COO_2)_2$) was obtained by dehydration of commercial lead acetate trihydrate (Prolabo) at 120°C under primary vacuum. In a typical experiment, 3.17 g of sodium (0.138 mole) were dissolved in 250 ml of propanol-2. Then, 26.9 g of anhydrous lead acetate (0.083 mole) was added and refluxed with strong mechanical stirring for 3 days under anhydrous conditions. After cooling, the solution was rapidly filtered. Gravimetric titration of its lead content with sulfuric acid yielded an amount of 0.071 mole of lead in the solution. This corresponds to the complete reaction (38):

$$2\,Na(OC_3H_7) + Pb(CH_3CO_2)_2 \rightarrow 2\,Na(CH_3CO_2) + Pb(OC_3H_7)_2.$$

To this solution of lead alkoxide (0.25 *M* in Pb) the appropriate amount of zirconium isopropoxide ($Zr(C_3H_7O)_4 \cdot C_3H_7OH$, Alfa Products, used as received) was added. The solution was refluxed for 1 hr before hydrolysis. Two experiments were performed. In the first experiment (A), water in isopropanol (4 *M*) was added in the ratio $[H_2O]/[Pb] = 4$; the precipitate was filtered and washed with dry isopropanol. In the second (B), a large excess of pure water was added; the precipitate was filtered and washed with pure hot water. Both powders were dried at 60°C overnight. Chemical analysis performed at the CNRS analysis facility in Vernaison indicates a Pb/Zr ratio of 1.00 ± 0.05 and only traces of sodium.

The precipitates have been studied by thermogravimetric analysis. As expected, some residual organics are found in powder (A) as demonstrated by the large and exothermic weight loss (Fig. 1a). Only a smooth endothermic weight loss associated with the decomposition of hydroxides is observed in the case of precipitate (B).

2.2. Structural Characterization of the Fully Hydrolyzed Material (B)

After drying and heating to 400°C, X-ray diffraction (Cu$K\alpha$, Bragg–Brentano geometry) indicates that powder (B) is amorphous (Fig. 2a). Upon heating at 500°C for 1 hr, a poorly crystalline material is obtained (Fig. 2b). Hereafter, it will be denoted Pb–ZrO_2. The X-ray pattern of tetragonal ZrO_2, obtained by hydrolysis of zirconium isopropoxide and heating at 400°C, is shown for comparison (Fig. 2c). The width of the peaks of Pb–ZrO_2 corresponds to a coherence domain of about 5 nm. The broad peaks have been indexed in a cubic cell (a = 5.25 Å) with a cell parameter in good agreement with the results of Yamagushi *et al.* (37) (c = 5.28 Å) and clearly different from pure ZrO_2. This indicates that a mixed structure is formed which must contain lead oxide. Above 550°C the phase slowly transforms within hours to the perovskite phase, which can be obtained as a pure phase after heating at 600°C for 16 hr (Fig. 2d). No phase separation into lead and zirconium oxide is observed.

To further investigate the relative distribution of Pb and Zr inside the structure, the material obtained at 500°C has

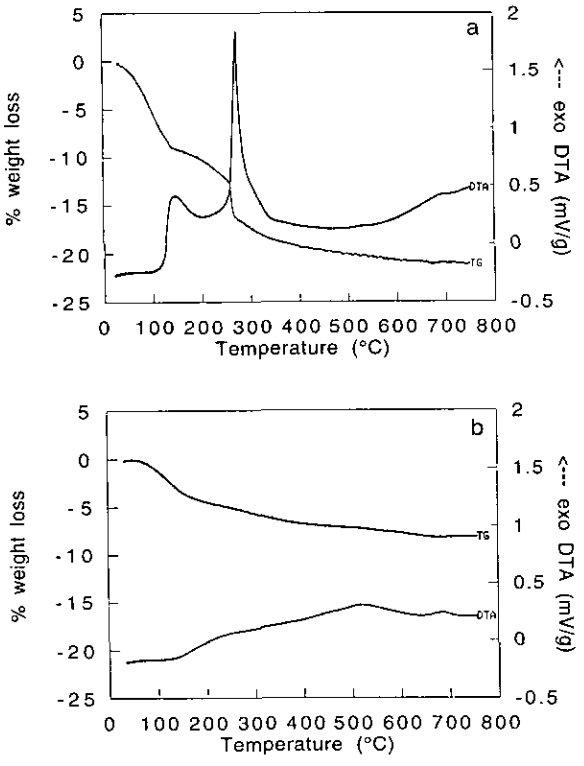

FIG. 1. Thermal analysis of Pb–Zr precipitates obtained by hydrolysis with (a) a ratio $H_2O/Pb = 4$; (b) a large excess of water.

been characterized by X-ray absorption spectroscopy at the Zr *K*–edge. It has been compared to yttrium-stabilized cubic ZrO_2 and monoclinic ZrO_2. Spectra have been recorded at the LURE synchrotron facility (Orsay, France) using the EXAFS I spectrometer equipped with a silicon (311) channel-cut monochromator. Operating conditions

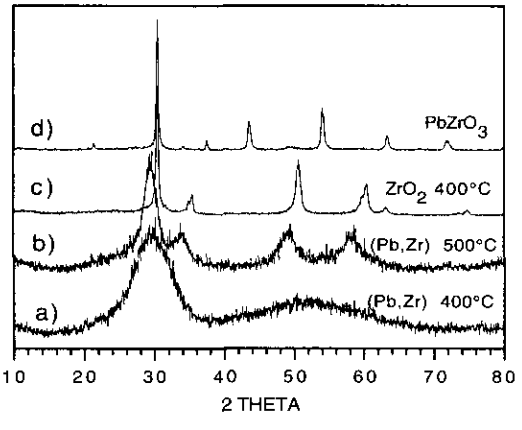

FIG. 2. X-ray diffraction pattern (Cu$K\alpha$ radiation) of (a) (Pb,Zr) precipitate heated at 400°C; (b) (Pb,Zr) precipitate heated at 500°C (Pb–ZrO_2 phase); (c) Zr precipitate heated at 400°C; (d) (Pb,Zr) precipitate heated at 600°C for 16 hr.

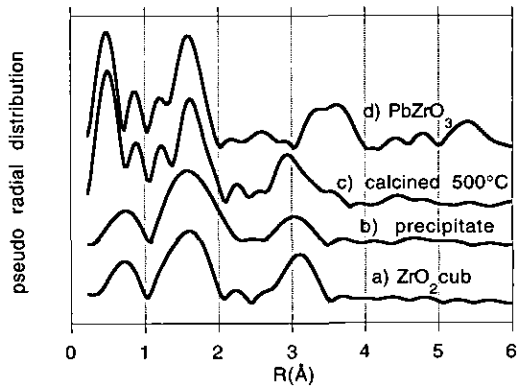

FIG. 3. Fourier transform of the k^3-weighted EXAFS spectra of: (a) cubic ZrO_2; (b) (Pb–Zr) precipitate as dried; (c) (Pb–Zr) precipitate heated at 500°C (Pb–ZrO_2 phase); and (d) $PbZrO_3$.

and data analysis of the absorption spectra are similar to those reported elsewhere (39).

EXAFS spectra have been transformed and studied using the software written by Michalowicz (40). The spectrum deconvolution is always the same: the background absorption is approximated from the pre-edge region using a straight line and atomic absorption is fitted between 18,060 and 18,950 eV with a 5th degree polynom. EXAFS signals are then extracted using the Lengeler–Eisenberger algorithm. The Fourier transform $F(R) = TF(k^3 \cdot \chi(k))$ of the k^3-weighted experimental EXAFS signal is performed between 1 and 12 $Å^{-1}$ using a Kaiser window ($\tau = 2.5$). These Fourier transforms give a pseudoradial distribution function that, in a first approach, can be considered as the distribution of neighboring atoms around Zr atoms, after addition of a phase correction (Fig. 3). Theoretical phase shift and backscattering amplitude functions are obtained from calculations by McKale *et al.* (41).

The simulation of the EXAFS oscillations corresponding to the first peak of the Fourier transform (between 1 and 2.2 Å) yield the zirconium–oxygen distances within the first coordination shell. The results for the different materials are reported in Table 1. In the case of monoclinic ZrO_2, two distances can be distinguished but in order to compare with other samples, a single distance is used in the fitting procedure. The resulting zirconium–oxygen distance for this compound is 2.19 Å, slightly higher than the average distance given by the structural data (three oxygen atoms at 2.07 Å and four at 2.21 Å; $\langle Zr–O \rangle = 2.15$ Å (43)) and by the EXAFS results of Catlow *et al.* (2.16 Å) (42). But in this way, the fits on all samples including monoclinic ZrO_2 give a zirconium–oxygen distance with a similar Debye–Waller coefficient ($\sigma \approx 0.09$ Å), which indicates a broad radial distribution of oxygen atoms. In the fits, the electron mean free path was fixed and the coordination number allowed to float. However, this gives

TABLE 1
Results of Fitting of EXAFS Data

Compound	Coordination number	Radial distance (Å)	Debye–Waller coefficient (σ) (Å)
Monoclinic ZrO_2	7.00[a]	2.19	0.085
Cubic Y–ZrO_2	7.12[b]	2.18	0.10
(Pb,Zr) RT	11.5[b]	2.18	0.11
(Pb,Zr) 400°C	8.4[b]	2.17	0.10
Pb–ZrO_2 500°C/1 hr	12.0[b]	2.16	0.12
$PbZrO_3$	8.34[b]	2.14	0.085

Note. For all samples, the electron mean free path (λ) was set to k/Γ with $\Gamma = 1.41$ Å^{-2}.

[a] Fixed value.

[b] Allowed to float during the fitting procedures.

poor and unrealistic results, as shown in Table 1. Small changes in the electron mean free paths strongly affect the coordination number. The only reliable information is actually the radial distance.

The radial distance of 2.165 Å for the Pb-ZrO_2 phase is similar to that observed (2.185 Å) for cubic ZrO_2. This distance corresponds in both cases to a seven- or eightfold oxygen coordination around zirconium. Shorter distances (2.14 Å) are observed in the $PbZrO_3$ perovskite in which zirconium has a sixfold coordination.

In the region between 2 and 4 Å, a second peak is observed. In cubic ZrO_2, this peak corresponds to an average Zr–Zr distance of 3.5 Å ($\sigma \approx 0.12$ Å). Filtering of the spectra is performed by operating an inverse Fourier transform limited to the data between 2 and 4 Å. The filters are reproduced in Fig. 4. They demonstrate the strong similarity of the EXAFS oscillations between cubic Y–ZrO_2 and the 500°C crystallized Pb–ZrO_2.

From the theoretical calculations of backscattering phase and amplitude functions, Pb and Zr backscatterers should be easily distinguishable, whereas Y and Zr have the same backscattering properties. Thus the strong similarity between the radial distributions of Y–ZrO_2 and Pb–ZrO_2 phase seems at first to indicate, that no lead is observed in the second coordination shell of Zr in the Pb–ZrO_2 phase. But this offers an apparent discrepancy with the X-ray diffraction results that show a Pb–ZrO_2 structure with a cell parameter much larger than the pure zirconium oxide. On the other hand, in these disordered materials with a wide range of distances between zirconium and its neighbors, EXAFS may fail to discriminate the backscattering contributions of Pb and Zr. Also, destructive interference of backscattering electronic wavefunctions has been described in the EXAFS spectra of tetragonal zirconia (44). Such effects may account for the absence of any contribution from lead backscatterers. No conclusion can be drawn from this EXAFS study.

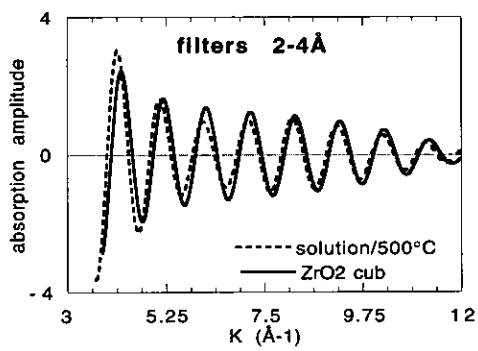

FIG. 4. Filtered (2–4 Å) EXAFS contributions for the (Pb–Zr) precipitae heated at 500°C (Pb–ZrO_2) and cubic ZrO_2.

Thus, the Pb–ZrO_2 cubic structure has been investigated by transmission electron microscopy (TEM). The TEM observations have been directly achieved on powders deposited on carbon-film-coated grids. The study has been carried out with a Topcon 002B electron microscope (200 kV) equipped with an energy dispersive spectroscopy X-ray analyzer (EDS, Kevex).

The Pb–ZrO_2 sample appears to be composed of small grains having a particle size of 5 nm (Fig. 5). Its electron diffraction pattern corresponds to the cubic structure observed in the X-ray diagram. No amorphous phase is observed in the picture and no diffusion ring corresponding to an amorphous phase is observed in the diffraction pattern. Therefore, one can estimate that less than 10–15% of the elements can be found in amorphous domains. Semiquantitative X-ray analysis indicates a homogeneous composition (Zr 65 ± 5%, Pb 35 ± 5%) down to a probe diameter as low as 5 nm, i.e., the size of a crystallite. This demonstrates that homogeneity has been achieved in this system and that it leads to the crystallization of a CaF_2-derived average structure.

2.3. *Effects of Residuals Organics*

The powder (A) obtained with a lower hydrolysis ratio is also amorphous. If a small amount of sample (100 mg) is slowly heated (300°C/hr) to 600°C and rapidly cooled, the cubic Pb–ZrO_2 phase is obtained in the presence of the $PbZrO_3$ perovskite (Fig. 6a). The perovskite would crystallize as a pure phase only after heating for hours at 600°C. But the results are strongly dependent on the heating rate, the mass of the sample, and the oxygen pressure, which controls the decomposition of organics between 200 and 400°C, as observed in the thermal analysis. When a larger mass of starting material (400 mg) is heated in the same way (Fig. 6b), some PbO is observed (both orthorhombic and tetragonal phases). Moreover, when the same amount of powder is directly placed into the hot furnace, a complete phase partitioning between PbO and poorly crystallized ZrO_2 is observed (Fig. 6c).

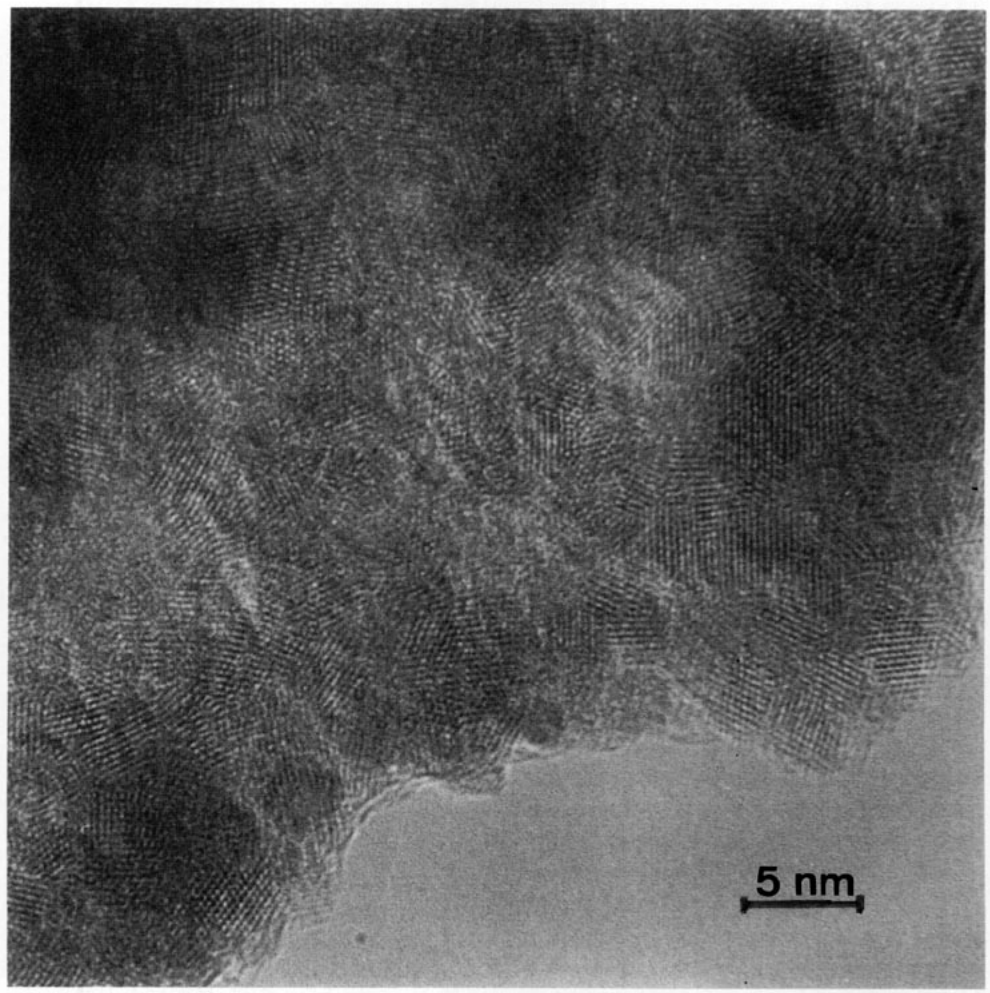

FIG. 5. High resolution transmission electron microscopy of the (Pb–Zr) precipitate heat-treated at 500°C for 1 hr (Pb–ZrO_2).

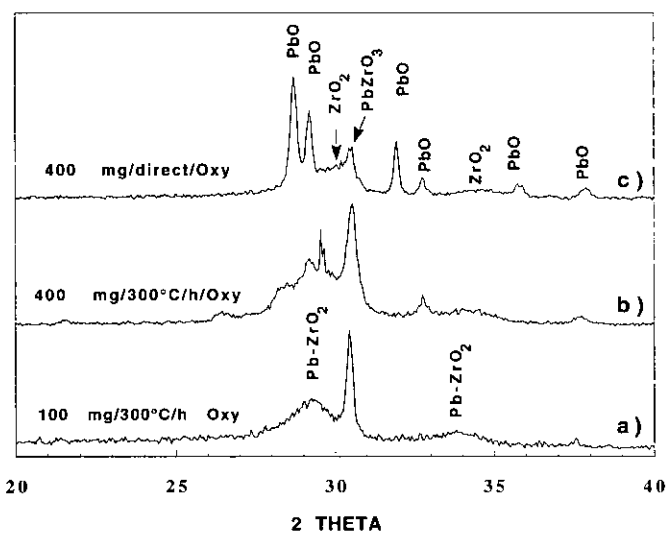

FIG. 6. X-ray diffraction patterns of powders heat-treated at various rates and for differents weights (Cu$K\alpha$ radiation).

This demonstrates the effect of residual organics and of the heating rate on the loss of homogeneity during the calcination step. Dried precipitates should not have any by-products, such as organics, because their exothermic decomposition may be responsible for phase separation and loss of homogeneity. The same conclusion has already been reached by Huling and Messing with regard to the synthesis of mullite from molecular precursors (18, 19). They have concluded that calcination should be limited to a temperature where only volatile species are mobile unless phase separation should occur.

As a conclusion of this experimental study, we confirm the results by Yamagushi *et al.* who have produced homogeneous Pb–ZrO_2 phases (37). The synthesis of this phase is very sensitive to the process and the Pb–ZrO_2 phase appears metastable as compared to phase separation at higher temperatures or during too rapid a calcination at low temperatures. This explains why there has been no report of a solid solution between PbO and ZrO_2 phases in the phase diagrams determined at high temperatures

(45) or by coprecipitation techniques and heat treatment at 650°C (46).

GENERAL CONCLUSION

Most of the studies in the domain of solution processes have been focusing on precursor chemistry as the art of tailoring ceramics. But homogeneity, although important, is not the only aspect of the synthesis and we have tried, for some examples given in this work, to demonstrate that the calcination and heating must be studied from a mechanistic point of view. Recent discussions have offered a starting point for these studies (5, 12, 18). We also believe that most of the understanding of the phase formation can be found in the metastable phases or mixtures occurring during the heating process. The structural defects that result from low-temperature synthesis offer also a clue to the way the phase formed. Another approach that we have not yet mentioned is the study of crystallization kinetics, which would also yield valuable information on phase nucleation and growth.

REFERENCES

1. J. Livage, M. Henry, and C. Sanchez, *Prog. Solid State Chem.* **18,** 259 (1988).
2. C. J. Brinker and G. W. Scherrer, "Sol–Gel Science" Academic Press, San Diego, 1990.
3. G. H. Yi and M. Sayer, *Am. Ceram. Soc. Bull.* **70,** 1173 (1991).
4. K. G. Caulton and L. G. Hubert-Pfalzgraf, *Chem. Rev.* **90,** 969, (1990).
5. C. D. Chandler, C. Roger, and M. J. Hampden-Smith, *Chem. Rev.* **93,** 1205 (1993).
6. C. D. Chandler and M. J. Hampden-Smith, *Chem. Mater.* **4,** 1137 (1992).
7. S. Hirano, T. Yogo, K. Kikuta, K. Kato, W. Sakamoto, and S. Ogasahara, *Ceram. Trans.* **25,** 19 (1992).
8. F. Chaput and J. P. Boilot, *J. Mater. Sci. Lett.* **6,** 1110 (1987).
9. S. P. Faure, P. Barboux, P. Gaucher, and J. Livage, *J. Mater. Chem.* **2,** 713 (1992).
10. P. Barboux *et al.*, unpublished results.
11. G. Guzman, P. Barboux, J. Livage, and J. Perrière, *Sol–Gel Sci. Technol.* **2,** 619 (1994).
12. F. F. Lange, M. L. Balmer, and C. G. Levi, *Sol–Gel Sci. Technol.* **2,** 317 (1994).
13. P. Barboux, J. M. Tarascon, L. H. Greene, G. W. Hull, and B. G. Bagley, *J. Appl. Phys.* **63,** 2725 (1988).
14. P. Barboux, I. Campion, S. Daghish, J. Livage, J. L. Genicon, A. Sulpice, and R. Tournier, *J. Non-Cryst. Solids* **147/148,** 704 (1992).
15. A. Hamdi, J. V. Mantese, A. H. Micheli, R. C. Laugal, and D. F. Dungan, *Appl. Phys. Lett.* **51,** 2152 (1987).
16. J. Chen, K. R. Udayakumar, K. G. Brooks, and L. E. Cross, *J. Appl. Phys.* **71,** 4465 (1992).
17. P. Barboux, J. M. Tarascon, F. Shokoohi, B. J. Wilkens, and C. L. Schwartz, *J. Appl. Phys.* **64,** 6382 (1988).
18. J. C. Huling and G. L. Messing, *J. Non-Cryst. Solids* **147/148,** 213 (1992).
19. J. C. Huling and G. L. Messing, *J. Am. Ceram. Soc.* **74,** 2374 (1991).
20. L. Bonhomme-Coury, N. Lequeux, S. Mussotte, and P. Boch, *Sol-Gel Sci. Technol.* **2,** 371 (1994).
21. J. Takahashi, N. Kakuta, and A. Ueno, *Mater. Res. Bull.* **26,** 243 (1991).
22. T. Novet and D. C. Johnson, *J. Am. Chem. Soc.* **113,** 3398 (1991).
23. L. Fister, D. C. Johnson, and R. Brown, *J. Am. Chem. Soc.* **116,** 629 (1994).
24. M. Lejeune and J. P. Boilot, *Ceram. Int.* **8,** 99 (1982).
25. S. Y Chen, C. M Wang, and S. Y Cheng, *J. Am. Ceram. Soc.* **74,** 2506 (1991).
26. S. L. Swartz and T. R. Shrout, *Mater. Res. Bull.* **17,** 1245 (1982).
27. L. F. Francis and D. A. Payne, *Mater. Res. Soc. Symp. Proc.* **200,** 173 (1990).
28. S. A. Khan, P. Barboux, B. G. Bagley, and F. E. Torres, *J. Non-Cryst. Solids* **110,** 142 (1989).
29. J. M. Heintz, M. Sanz, E. Marquestaut, J. Etourneau, and J. P. Bonnet, *J. Am. Ceram. Soc.* **74,** 998 (1991).
30. V. Caignaert, M. Hervieu, J. Wang, G. Desgardins, B. Raveau, F. Boterel, and J. M. Hausonne, *Physica C* **170,** 139 (1990).
31. F. J. Gotor, P. Odier, M. Gervais, and J. Choisnet, *Sol-Gel Sci. Technol.* **2,** 427 (1994).
32. E. Rossen, J. N. Reimers, and J. R. Dahn, *Solid State Ionics* **62,** 53 (1993).
33. R. J. Gummow, M. M. Thackeray, W. I. F. David, and S. Hull, *Mater. Res. Bull.* **27,** 327 (1992).
34. B. Garcia, P. Barboux, F. Ribot, A. Khan-Harari, L. Mazerolles, J. Pereira-Ramos, and N. Baffier, *Solid State Ionics*, in press (1995).
35. K. T. Jacob and W. W. Schim, *J. Am. Ceram. Soc.* **64,** 573 (1981).
36. L. G. Hubert-Pfalzgraf, *Mater. Res. Soc. Symp. Proc.* **271,** 15 (1992).
37. O. Yamagushi, T. Fukuoka, and Y. Kawakami, *J. Mater. Sci. Lett.* **9,** 958 (1990).
38. R. Papiernik, L. G. Hubert-Pfalzgraf, and M. C. Massiani, *Polyhedron* **10,** 1657 (1991).
39. F. Ribot, P. Toledano, and C. Sanchez, *Chem. Mater.* **3,** 759 (1991).
40. A. Michalowicz, "EXAFS pour le Mac, Logiciels pour la Chimie." Société Française de Chimie, Paris, 1991.
41. A. G. McKale, B. W. Veal, A. P. Paulikas, S. K. Khan, and G. S. Knapp, *J. Am. Chem. Soc.* **110,** 3763 (1988).
42. C. R. A. Catlow, A. V. Chadwick, G. N. Greaves, and L. M. Moroney, *J. Am. Ceram. Soc.* **69,** 272 (1986).
43. C. Landron, D. Ruffier, B. Dubois, P. Odier, D. Bonnin, and H. Dexpert, *Phys. Status Solidi* **121,** 359 (1990).
44. T. Dumas, A. Ralos, M. Gandais, and J. Petiau, *J.Mater. Sci. Lett.* **4,** 129 (1985).
45. S. Fushimi and T. Ikeda, *J. Am. Ceram. Soc.* **50,** 131 (1967).
46. H. J.Stöcker, Thèse de l'Université Paris, 1960.